SCALAR DAMAGE BASED ON MICROPOLAR CONTINUA – MESH-FREE APPROXIMATION

Lapo Gori

Marcella Passos Andrade

Ramon Pereira da Silva

Samuel Silva Penna

Roque Luiz da Silva Pitangueira

lapo@dees.ufmg.br, marcella@dees.ufmg.br, ramon@ufmg.br

spenna@dees.ufmg.br, roque@dees.ufmg.br

Department of Structural Engineering, Federal University of Minas Gerais (UFMG)

Avenida Antônio Carlos, 6627, Pampulha, 31270-901, Belo Horizonte, MG, Brasil

*Abstract. Recently, scalar damage models based on the micropolar continuum theory have been proposed, in order to represent the physically non-linear behaviour of quasi-brittle materials. Due to its regularization properties, widely investigated in elasto-plasticity, the micropolar theory represents a valid alternative for mitigating pathological phenomena that arise in the numerical simulations. In the last years, also the class of mesh-free methods have been shown to be capable to regularize the response of problems where localization occours. This paper investigates the coupling of micropolar damage models with mesh-free methods, with specific attention on the Element Free Galerkin (EFG) method. The micropolar theory is presented in a tensorial generalized form, and different scalar damage models are derived in a theoretical and computational unified framework for constitutive models. The computational aspects of the coupling between micropolar damage and mesh-free approach are also discussed, with specific attention on the implementation in the **INSANE** (INteractive Structural ANalysis Enviroment) system. Numerical simulations are presented in order to illustrate the proposed models.*

Keywords: Micropolar continua, Scalar damage, Strain localization, Mesh-free methods, Element Free Galerkin

1   INTRODUCTION

In the past, *micropolar* (or Cosserat) media (Cosserat and Cosserat, 1909) have been widely investigated, mainly due to the regularization effects that such models are able to introduce in the numerical simulations where localization occours. Regarding the physically non-linear analysis, despite the wide number of applications of the micropolar theory to elasto-plasticity (see, e.g., de Borst and Sluys (1991); Sluys (1992); de Borst (1993); Iordache and Willam (1998); Bauer et al. (2012)), only a few works are devoted to its combination with damage models (Steinmann, 1995; Rahaman et al., 2015; Xotta et al., 2016). Recently, a more general theoretical and computational framework for micropolar elasto-plasticity and damage, based on a unified formulation, has been proposed (Gori et al., 2015a,b,c, 2016). Regarding the numerical investigations on micropolar media, these are mainly based on finite element models, with a few applications to different numerical methods (see, e.g., Liang and Huang (1996); Rahaman et al. (2015)).

Recently, it has been shown that, due to their analogy with non-local models, some classes of *mesh-free* methods, like *moving least square*, *reproducing kernel* approximations, and methods based on *strain smoothing*, are able to bring regularization effects on localization problems (Liu et al., 1999; Chen et al., 2000; Li et al., 2000; Li and Liu, 2000; Chen et al., 2004, 2007; Wang and Li, 2012; Pozo et al., 2014). This is due to the fact that the approximation functions are not constructed locally, because of the use of weighting functions which support size is greater than the nodes spacing; hence, a *non-locality* is embedded in the numerical discretization. However, as pointed out in the cited works, the regularization introduced by mesh-free methods is not effective in all the situations, hence it should be combined with other regularization techniques.

In this paper, the micropolar scalar damage formulation presented in Gori et al. (2015c, 2016) is enriched with damage models derived from the original Mazars model (Mazars and Cabot, 1989), adapted to the micropolar theory. The proposed models are analized within the context of the *Element Free Galerkin* (EFG) approximation (Belytschko et al., 1994), representing to the authors knowledge one of the first applications of the micropolar theory to such a numerical method. The first part of the paper recalls the basic equations of the micropolar theory, together with some details on its Voigt representation, that will be used throughout the numerical formulation. The main aspects of the unified scalar damage formulation are then briefly resumed, and the proposed damage models are formulated. The problem is then discretized using an extention to the micropolar theory of the EFG approximation with the Lagrange multipliers method for essential boundary conditions imposition. The proposed models have been implemented in the software **INSANE** (INteractive Structural ANalysis Environment (INSANE Project, 2016)), taking advantage of the existing implementation of the EFG method (Silva, 2012) and of the linear algebra library *SuiteSparse* (Davis, 2004, 2006) implemented by Andrade and Silva (2015). Finally, numerical simulations are presented in order to illustrate the proposed models and their combination with the meshfree approach.

1.1   Notations

Some standard notations used in the body of the paper are summarized here. The symbol $\mathbf{D} \subseteq \mathbf{E}$ indicates the domain of the body, i.e., a subset of the three-dimensional Euclidean space $\mathbf{E}$, in which the orthonormal basis $(\bar{e}_i)$ is defined. *Vectors* are indicated as $\bar{x} = x_i\,\bar{e}_i$, while

second-order and *fourth-order* tensors respectively as $\underline{\mathbf{x}} = x_{ij}\,\bar{e}_i \otimes \bar{e}_j$, and $\hat{\mathbf{x}} = x_{ijk\ell}\,\bar{e}_i \otimes \bar{e}_j \otimes \bar{e}_k \otimes \bar{e}_\ell$. The symbol $\cdot$ denotes both the standard dot product between vectors and the total contraction between tensors like, for example, $\bar{x} \cdot \bar{y} = x_i\,y_i$, $\underline{\mathbf{x}} \cdot \bar{y} = x_{ij}\,y_j\,\bar{e}_i$, $\hat{\mathbf{x}} \cdot \underline{\mathbf{y}} = x_{ijk\ell}\,y_{k\ell}\,\bar{e}_i \otimes \bar{e}_j$ and the other possible combinations. With the symbol $\otimes$ the standard tensorial product, as $\bar{x} \otimes \bar{y} = x_i\,y_j\,\bar{e}_i \otimes \bar{e}_j$ or $\underline{\mathbf{x}} \otimes \underline{\mathbf{y}} = x_{ij}\,y_{k\ell}\,\bar{e}_i \otimes \bar{e}_j \otimes \bar{e}_k \otimes \bar{e}_\ell$, is indicated. In the following of the paper, if not differently specified, spaces will be assumed to be three-dimensional and the latin indexes will run from 1 to 3. In the case of *generalized* quantities, defined in six-dimensional spaces, greek letters will be used to indicate indexes running from 1 to 6. In some applications, in order to simplify the treatise, the Voigt notation will be used to represent second-order and fourth-order tensors; once a certain coordinates system has been fixed, a generic second-order tensor $\underline{\mathbf{x}}$ with dimension three can be represented by means of an *array* with nine components, indicated with the symbol $\{\underline{\mathbf{x}}\}$. In an analogus way, a fourth-order tensor $\hat{\mathbf{x}}$ with dimension three can be represented by means of a 9×9 matrix, indicated as $[\hat{\mathbf{x}}]$. The same symbols $\{\cdot\}$ and $[\cdot]$ are also used in section 4 to indicate, respectively, arrays and matrices in numerical equations.

2 MICROPOLAR CONTINUUM THEORY

Micropolar continua belong to the family of *multi-field* continua, i.e., continuum bodies which configuration is defined by two descriptors, the *motion* of the material points of the body and a *morphological descriptor* (see, e.g., Mariano and Stazi (2005) for further details). In the peculiar case of the micropolar continuum, such a morphological descriptor corresponds to a *rigid rotation* of the material points of the continuum.

In a geometrically linear approach, at each point of the continuum, a *displacement field* $\bar{u}$ and a *micro-rotation field* $\bar{\varphi}$ can be defined, leading to the following strain measures

$$\underline{\gamma} = \mathrm{grad}^{\mathrm{T}}(\bar{u}) - \mathsf{e} \cdot \bar{\varphi} = (u_{j,i} - \mathsf{e}_{ijk}\,\varphi_k)\,\bar{e}_i \otimes \bar{e}_j \tag{1}$$

$$\underline{\kappa} = \mathrm{grad}^{\mathrm{T}}(\bar{\varphi}) = \varphi_{j,i}\,\bar{e}_i \otimes \bar{e}_j \tag{2}$$

which are referred to, respectively, as *strain tensor* and *micro-curvature tensor*, and where e represents the standard *Levi-Civita* symbol with three indexes. To these strain measures correspond, respectively, the stress tensor $\underline{\sigma}$ and the couple-stress tensor $\underline{\mu}$, which must satisfy the local equilibrium equations for forces and moments in the domain $\mathbf{D}$

$$\mathrm{div}^{\mathrm{T}}(\underline{\sigma}) + \bar{b} = \bar{0} \longrightarrow (\sigma_{ij,i} + b_j)\,\bar{e}_j = \bar{0} \tag{3}$$

$$\mathrm{div}^{\mathrm{T}}(\underline{\mu}) + \mathsf{e} \cdot \underline{\sigma} + \bar{l} = \bar{0} \longrightarrow (\mu_{ij,i} + \mathsf{e}_{jkl}\,\sigma_{kl} + l_j)\,\bar{e}_j = \bar{0} \tag{4}$$

where $\bar{b}$ and $\bar{l}$ represent, respectively, volume forces and volume couples acting in the body domain. To the previous equations, the following *natural* and *essential* boundary conditions are associated

$$\bar{n} \cdot \underline{\sigma} = \bar{t}_A \quad \text{at} \quad \partial\mathbf{D}_n^u, \quad \bar{n} \cdot \underline{\mu} = \bar{t}_C \quad \text{at} \quad \partial\mathbf{D}_n^\varphi \tag{5}$$

$$\bar{u} = \bar{u}^* \quad \text{at} \quad \partial\mathbf{D}_e^u, \quad \bar{\varphi} = \bar{\varphi}^* \quad \text{at} \quad \partial\mathbf{D}_e^\varphi \tag{6}$$

where $\bar{n}$ is the unit outward normal to the boundary $\partial\mathbf{D}$, which parts are such that

$$\partial\mathbf{D}_n^u \cap \partial\mathbf{D}_e^u = \emptyset, \quad \partial\mathbf{D}_n^u \cup \partial\mathbf{D}_e^u = \partial\mathbf{D}, \quad \partial\mathbf{D}_n^\varphi \cap \partial\mathbf{D}_e^\varphi = \emptyset, \quad \partial\mathbf{D}_n^\varphi \cup \partial\mathbf{D}_e^\varphi = \partial\mathbf{D} \tag{7}$$

In the field of elasticity, the different stress and strain measures are related by the following constitutive equations

$$\underline{\sigma} = \hat{\mathbf{A}}^0 \cdot \underline{\gamma} \tag{8}$$

$$\underline{\mu} = \hat{\mathbf{C}}^0 \cdot \underline{\kappa} \tag{9}$$

where $\hat{\mathbf{A}}^0$ and $\hat{\mathbf{C}}^0$ are the elastic constitutive operators for the micropolar continuum theory.

It should be noted that the components of the micro-curvature tensor $\underline{\kappa}$ and of the couple-stress tensor $\underline{\mu}$ are not characterized by the same units of measure of, respectively, the strain tensor $\underline{\gamma}$ and the stress tensor $\underline{\sigma}$. In a number of applications it is convenient to scale such operators in order to obtain a dimensional compatibility. The micro-curvature and couple-stress tensors are then replaced by the scaled operators $\underline{\kappa}^*$ and $\underline{\mu}^*$ defined as $\underline{\kappa}^* = \hat{\mathbf{L}} \cdot \underline{\kappa}$ and $\underline{\mu}^* = \hat{\mathbf{L}}^{-1} \cdot \underline{\mu}$, where $\hat{\mathbf{L}}$ is a fourth-order tensor containing the characteristic lengths of the micropolar medium. The constitutive relation for the scaled operators, analogous to the one of Eq. (9), is expressed as $\underline{\mu}^* = \hat{\mathbf{C}}^{*0} \cdot \underline{\kappa}^*$, with $\hat{\mathbf{C}}^{*0} = \hat{\mathbf{L}}^{-1} \cdot \hat{\mathbf{C}}^0 \cdot \hat{\mathbf{L}}^{-1}$.

2.1 Weak form

Following the standard weighted residual method, the following weak form of the coupled boundary value problem that governs a micropolar medium can be obtained: find the fields $\bar{u} \in \mathcal{U}$ and $\bar{\varphi} \in \mathcal{V}$ such that

$$\int_{\mathbf{D}} \mathrm{grad}^{\mathrm{T}}(\bar{w}) \cdot \left(\hat{\mathbf{A}}^S \cdot \mathrm{grad}^{\mathrm{T}}(\bar{u}) \right) \, d\mathcal{V} + \int_{\mathbf{D}} \mathrm{grad}^{\mathrm{T}}(\bar{w}) \cdot \left(\hat{\mathbf{A}}^S \cdot (-\mathbf{e} \cdot \bar{\varphi}) \right) \, d\mathcal{V} + \tag{10}$$

$$- \int_{\partial \mathbf{D}_n^u} \bar{w} \cdot \bar{t}_A \, d\mathcal{A} - \int_{\mathbf{D}} \bar{w} \cdot \bar{b} \, d\mathcal{V} = 0, \quad \forall \bar{w} \in \mathcal{U}^0$$

$$\int_{\mathbf{D}} \mathrm{grad}^{\mathrm{T}}(\bar{\omega}) \cdot \left(\hat{\mathbf{C}}^S \cdot \mathrm{grad}^{\mathrm{T}}(\bar{\varphi}) \right) \, d\mathcal{V} - \int_{\mathbf{D}} \bar{\omega} \cdot \left(\mathbf{e} \cdot \left(\hat{\mathbf{A}}^S \cdot \mathrm{grad}^{\mathrm{T}}(\bar{u}) \right) \right) \, d\mathcal{V} + \tag{11}$$

$$- \int_{\mathbf{D}} \bar{\omega} \cdot \left(\mathbf{e} \cdot \left(\hat{\mathbf{A}}^S \cdot (-\mathbf{e} \cdot \bar{\varphi}) \right) \right) \, d\mathcal{V} - \int_{\partial \mathbf{D}_n^\varphi} \bar{\omega} \cdot \bar{t}_C \, d\mathcal{A} - \int_{\mathbf{D}} \bar{\omega} \cdot \bar{l} \, d\mathcal{V} = 0, \quad \forall \bar{\omega} \in \mathcal{V}^0$$

where $\mathcal{U}$ and $\mathcal{V}$ are the spaces of *trial functions*, and $\mathcal{U}^0$ and $\mathcal{V}^0$ are the spaces of *test functions*, defined as

$$\mathcal{U} := \left\{ \bar{u} | \bar{u} \in \mathbf{H}^1(\mathbf{D}), \bar{u} = \bar{u}^* \text{ at } \partial \mathbf{D}_e^u \right\}, \qquad \mathcal{V} := \left\{ \bar{\varphi} | \bar{\varphi} \in \mathbf{H}^1(\mathbf{D}), \bar{\varphi} = \bar{\varphi}^* \text{ at } \partial \mathbf{D}_e^\varphi \right\} \tag{12}$$

$$\mathcal{U}^0 := \left\{ \bar{w} | \bar{w} \in \mathbf{H}^1(\mathbf{D}), \bar{w} = \bar{0} \text{ at } \partial \mathbf{D}_e^u \right\}, \qquad \mathcal{V}^0 := \left\{ \bar{\omega} | \bar{\omega} \in \mathbf{H}^1(\mathbf{D}), \bar{\omega} = \bar{0} \text{ at } \partial \mathbf{D}_e^\varphi \right\} \tag{13}$$

where $\mathbf{H}^1(\mathbf{D})$ is an *Hilbert* space over the domain $\mathbf{D}$.

2.2 Voigt notation

The Voigt notation for the micropolar theory, that will be used in Sec. 4, is here briefly exposed for a plane-stress case. The displacement and micro-rotation fields are expressed as the arrays

$$\{\bar{u}\} = (u_x \, u_y)^T, \qquad \{\bar{\varphi}\} = \varphi_z \tag{14}$$

while stress and strain measures are expressed as

$$\{\underline{\sigma}\} = (\sigma_{xx}\ \sigma_{xy}\ \sigma_{yx}\ \sigma_{yy})^T, \qquad \{\underline{\gamma}\} = (\gamma_{xx}\ \gamma_{xy}\ \gamma_{yx}\ \gamma_{yy})^T \tag{15}$$

$$\{\underline{\mu}\} = (\mu_{xy}\ \mu_{yx})^T, \qquad \{\underline{\kappa}\} = (\kappa_{xy}\ \kappa_{yx})^T \tag{16}$$

The scaled couple-stress and micro-curvature tensors are related to the unscaled ones by

$$\{\underline{\mu}^*\} = (\mu_{xy}/L_f\ \mu_{yx}/L_f)^T, \qquad \{\underline{\kappa}^*\} = (\kappa_{xy}L_f\ \kappa_{yx}L_f)^T \tag{17}$$

where L_f is the *bending length* of the micropolar medium (see, e.g., de Borst and Sluys (1991)). Equations (1) and (2) are then rewritten as

$$\{\underline{\gamma}\} = [L_A]\{\bar{u}\} - [\mathrm{e}]\{\bar{\varphi}\} = \begin{pmatrix} \partial_x & 0 \\ 0 & \partial_x \\ \partial_y & 0 \\ 0 & \partial_y \end{pmatrix} \begin{pmatrix} u_x \\ u_y \end{pmatrix} - \begin{pmatrix} 0 \\ 1 \\ -1 \\ 0 \end{pmatrix} \varphi_z \tag{18}$$

$$\{\underline{\kappa}^*\} = [L_C^*]\{\bar{\varphi}\} = \begin{pmatrix} L_f\ \partial_x \\ L_f\ \partial_y \end{pmatrix} \varphi_z \tag{19}$$

where the derivative operator $[L_C^*]$ already embeds the characteristic bending length L_f.

3 SCALAR DAMAGE IN MICROPOLAR MEDIA

A scalar damage model based on the micropolar theory is characterized by the following total relations (Gori et al., 2015c, 2016)

$$\underline{\sigma} = (1 - D)\hat{\mathbf{A}}^0 \cdot \underline{\gamma} \tag{20}$$

$$\underline{\mu} = (1 - D)\hat{\mathbf{C}}^0 \cdot \underline{\kappa} \tag{21}$$

where D is a scalar *damage variable*, assumed to vary from 0 (undamaged material) to 1 (completely damaged material). Adopting the same compact *enhanced tensorial representation* already used in Gori et al. (2015c, 2016), the previous equations can be rewritten as

$$\underline{\Sigma} = (1 - D)\hat{\mathcal{E}}^0 \cdot \mathbf{\Gamma} \tag{22}$$

where the *generalized stress operator* $\underline{\Sigma}$ and the *generalized strain operator* $\mathbf{\Gamma}$, both represented by second-order tensors with dimension six, are defined by

$$\underline{\Sigma} = \begin{pmatrix} \sigma & \mathbf{0} \\ \mathbf{0} & \underline{\mu} \end{pmatrix}, \qquad \mathbf{\Gamma} = \begin{pmatrix} \gamma & \mathbf{0} \\ \mathbf{0} & \underline{\kappa} \end{pmatrix} \tag{23}$$

and where $\hat{\mathcal{E}}^0$ is a fourth-order tensor with dimension six containing the components of both $\hat{\mathbf{A}}^0$ and $\hat{\mathbf{C}}^0$.

The different phases of the loading process are described by a single loading function $f(\underline{\gamma}, \underline{\kappa}, D)$, depending on both the strain and micro-curvature tensors and on the scalar damage variable; in the specific case of a scalar damage model it assumes the expression

$$f(\underline{\gamma}, \underline{\kappa}, D) = g(\underline{\gamma}, \underline{\kappa}) - K(D) \leq 0 \tag{24}$$

where $g(\underline{\gamma}, \underline{\kappa})$ is a function depending only on the deformation, that represents the loading condition of the continuum and that is a characteristic of each peculiar model, while $K(D)$ is an historical parameter that depends on the damage variable. The historical parameter is representative of the maximum level of deformation reached during the loading process of the model.

Focusing on a strain-based approach for the scalar damage formulation, the stress and couple-stress rates can be additively decomposed into *elastic* and *degrading* parts as

$$\underline{\dot{\sigma}} = \underline{\dot{\sigma}}^e + \underline{\dot{\sigma}}^d \tag{25}$$

$$\underline{\dot{\mu}} = \underline{\dot{\mu}}^e + \underline{\dot{\mu}}^d \tag{26}$$

where the elastic parts $\underline{\dot{\sigma}}^e$ and $\underline{\dot{\mu}}^e$ are such that

$$\underline{\dot{\sigma}}^e = \hat{\mathbf{A}}^S \cdot \underline{\dot{\gamma}} \tag{27}$$

$$\underline{\dot{\mu}}^e = \hat{\mathbf{C}}^S \cdot \underline{\dot{\kappa}} \tag{28}$$

and the degrading parts $\underline{\dot{\sigma}}^d$ and $\underline{\dot{\mu}}^d$ are defined by the degradation rules

$$\underline{\dot{\sigma}}^d = \dot{\lambda}\, \underline{\mathbf{m}}_A^* = -\dot{\lambda}\, \hat{\mathbf{A}}^0 \cdot \underline{\gamma} = -\dot{\lambda}\, \underline{\sigma}^0 \tag{29}$$

$$\underline{\dot{\mu}}^d = \dot{\lambda}\, \underline{\mathbf{m}}_C^* = -\dot{\lambda}\, \hat{\mathbf{C}}^0 \cdot \underline{\kappa} = -\dot{\lambda}\, \underline{\mu}^0 \tag{30}$$

where $\dot{\lambda}$ is the *inelastic multiplier*, defining the magnitude of the inelastic rates, while the operators $\underline{\mathbf{m}}_A^*$ and $\underline{\mathbf{m}}_C^*$ represent, respectively, the *directions of degradations* of the stress and couple-stress rates.

Making use of these elements, from Eqs. (20) and (21), the following expressions for the stress and couple-stress rates can be obtained

$$\underline{\dot{\sigma}} = \left((1-D)\, \hat{\mathbf{A}}^0 - \frac{1}{\frac{\partial K}{\partial D}}\, \underline{\sigma}^0 \otimes \frac{\partial g}{\partial \underline{\gamma}} \right) \cdot \underline{\dot{\gamma}} - \left(\frac{1}{\frac{\partial K}{\partial D}}\, \underline{\sigma}^0 \otimes \frac{\partial g}{\partial \underline{\kappa}} \right) \cdot \underline{\dot{\kappa}} \tag{31}$$

$$\underline{\dot{\mu}} = \left((1-D)\, \hat{\mathbf{C}}^0 - \frac{1}{\frac{\partial K}{\partial D}}\, \underline{\mu}^0 \otimes \frac{\partial g}{\partial \underline{\kappa}} \right) \cdot \underline{\dot{\kappa}} - \left(\frac{1}{\frac{\partial K}{\partial D}}\, \underline{\mu}^0 \otimes \frac{\partial g}{\partial \underline{\gamma}} \right) \cdot \underline{\dot{\gamma}} \tag{32}$$

The previous expressions can be condensed into the equation

$$\underline{\dot{\Sigma}} = \hat{\mathcal{E}}^t \cdot \underline{\dot{\Gamma}} \tag{33}$$

introducing the *generalized tangent operator*

$$\hat{\mathcal{E}}^t = (1-D)\, \hat{\mathcal{E}}^0 - \frac{1}{\frac{\partial K}{\partial D}}\, \underline{\Sigma}^0 \otimes \frac{\partial f}{\partial \underline{\Gamma}} \tag{34}$$

with

$$\underline{\Sigma}^0 = \begin{pmatrix} \underline{\sigma}^0 & \mathbf{0} \\ \mathbf{0} & \underline{\mu}^0 \end{pmatrix}, \qquad \frac{\partial f}{\partial \underline{\Gamma}} = \begin{pmatrix} \frac{\partial f}{\partial \underline{\gamma}} & \mathbf{0} \\ \mathbf{0} & \frac{\partial f}{\partial \underline{\kappa}} \end{pmatrix} \tag{35}$$

3.1 Mazars damage model

From the previous general representation for scalar damage models based on the micropolar theory, specific constitutive models can be defined once the function $g(\underline{\gamma}, \underline{\kappa})$, usually known as *equivalent deformation*, and the damage function $D(\Gamma_{eq})$ are fixed.

An extention of the original Mazars damage model (Mazars, 1984) is proposed, represented by the equivalent deformation

$$\Gamma_{eq} := g(\underline{\gamma}, \underline{\kappa}) = \sqrt{\left[\sum_{k=1}^{3} \left(< \varepsilon^{(k)} >_+ \right)^2 \right] + \underline{\kappa}^* \cdot \underline{\kappa}^*} \tag{36}$$

where $\varepsilon^{(k)}$ is the k-th eigenvalue of the symmetric part of the strain tensor ($\underline{\varepsilon} = \underline{\gamma}^{sym}$), while the operator $< \cdot >_+$ indicates the positive part of a quantity

$$< \varepsilon^{(k)} >_+ = \frac{\varepsilon^{(k)} + |\varepsilon^{(k)}|}{2} \tag{37}$$

With this equivalent deformation, the gradients of the loading function, represented in Voigt notation, are expressed as

$$\left\{ \frac{\partial f}{\partial \underline{\gamma}} \right\}_g = \frac{1}{\Gamma_{eq}} \ [T_\varepsilon]^T < \{\underline{\varepsilon}\}_\ell >_+ \tag{38}$$

$$\left\{ \frac{\partial f}{\partial \underline{\kappa}^*} \right\}_g = \frac{1}{\Gamma_{eq}} \ \{\underline{\kappa}^*\}_g \tag{39}$$

where with the subscripts g and ℓ, the *global* coordinate system and the *local principal* system of the tensor $\underline{\varepsilon}$ are indicated, respectively, and where the matrix $[T_\varepsilon]$ represents the transformation matrix of the symmetric part of the strain tensor between the two systems, $\{\underline{\varepsilon}\}_\ell = [T_\varepsilon] \ \{\underline{\varepsilon}\}_g$.

As in the orginal work of Mazars, the damage variable is obtained as a combination of two different traction and compression damage variables

$$D := \alpha_t \, D_t + \alpha_c \, D_c \tag{40}$$

Such damage variables are defined as the following functions of the equivalent deformation

$$D_t(\Gamma_{eq}) := 1 - \frac{1}{\Gamma_{eq}} \, (1 - A_t) K_0 - \frac{1}{e^{B_t(\Gamma_{eq} - K_0)}} A_t \tag{41}$$

$$D_c(\Gamma_{eq}) := 1 - \frac{1}{\Gamma_{eq}} \, (1 - A_c) K_0 - \frac{1}{e^{B_c(\Gamma_{eq} - K_0)}} A_c \tag{42}$$

where K_0 is a threshold value for the equivalent deformation, representing the onset of damage, and where the parameters A_t, A_c, B_t and B_c assume the role of material parameters. The weighting functions α_t and α_c are evaluated as

$$\alpha_t := \sum_{k=1}^{3} H_k \frac{\varepsilon^t_{(k)}(\varepsilon^t_{(k)} + \varepsilon^c_{(k)})}{\Gamma^2_{eq}} \tag{43}$$

$$\alpha_c := \sum_{k=1}^{3} H_k \frac{\varepsilon^c_{(k)}(\varepsilon^t_{(k)} + \varepsilon^c_{(k)})}{\Gamma^2_{eq}} \tag{44}$$

where the terms $\varepsilon_{(k)}^{t}$ and $\varepsilon_{(k)}^{c}$ represent, respectively, the eigenvalues of the strain tensors $\underline{\varepsilon}^{t}$ and $\underline{\varepsilon}^{c}$ obtained using the positive and negative parts of the stress tensor $\underline{\sigma}^{0} = \hat{\mathbf{A}}^{0} \cdot \underline{\varepsilon}$, represented in its principal system

$$\underline{\sigma}^{0} = <\underline{\sigma}^{0}>_{+} + <\underline{\sigma}^{0}>_{-} \tag{45}$$

$$\underline{\varepsilon}^{t} := \left(\hat{\mathbf{A}}^{0}\right)^{-1} \cdot <\underline{\sigma}^{0}>_{+} \tag{46}$$

$$\underline{\varepsilon}^{c} := \left(\hat{\mathbf{A}}^{0}\right)^{-1} \cdot <\underline{\sigma}^{0}>_{-} \tag{47}$$

and where the parameters H_k are given by

$$H_k := \begin{cases} 1 & \text{if} \quad \varepsilon_{(k)}^{t} + \varepsilon_{(k)}^{c} \geq 0 \\ 0 & \text{if} \quad \varepsilon_{(k)}^{t} + \varepsilon_{(k)}^{c} < 0 \end{cases} \tag{48}$$

From Equation 40, the inverse of the post-critical modulus can be evaluated as

$$\frac{1}{H^{*}} = \frac{\partial D}{\partial K} = \frac{\partial D}{\partial \Gamma_{eq}} \frac{\partial \Gamma_{eq}}{\partial K} = \frac{\partial D}{\partial \Gamma_{eq}} \tag{49}$$

Simplified Mazars model

As suggested in de Borst and Gutiérrez (1999), the Mazars equivalent deformation (Eq. (36)) can be combined with different functions for the damage evolution rather than the one of Eq. (40), in order to obtain simplified models. In this case, a simplified model is obtained combining the equivalent deformation of Eq. (36) with the following exponential damage law

$$D(\Gamma^{eq}) = 1 - \frac{K_0}{\Gamma^{eq}} \left(1 - \chi + \chi e^{-\beta(\Gamma^{eq} - K_0)}\right) \tag{50}$$

where K_0 is a threshold value for the equivalent deformation, representing the onset of damage, and where χ and β are parameters that define, respectively, the maximum allowed damage level and the damage evolution intensity.

4   EFG APPROXIMATION

The problem described in the previous sections is discretized with an *Element Free Galerkin* (EFG) approximation, based on *Moving Least Square* (MLS) shape functions. Due to the lack of *delta Kronecker* property of such shape functions, the *Lagrange multipliers* method is adopted to impose *essential* boundary conditions (Eq. (6)), resulting in the following modified weak

form, directly expressed in Voigt notation

$$\int_{\mathbf{D}} ([L_A]\{\bar{w}\})^T \, [\hat{\mathbf{A}}] \, ([L_A]\{\bar{u}\}) \; d\mathcal{V} + \int_{\mathbf{D}} ([L_A]\{\bar{w}\})^T \, [\hat{\mathbf{A}}] \, (-[\mathrm{e}]\{\bar{\varphi}\}) \; d\mathcal{V} + \tag{51}$$

$$- \int_{\partial \mathbf{D}_n^u} \{\bar{w}\}^T \{\bar{t}_A\} \, d\mathcal{A} - \int_{\mathbf{D}} \{\bar{w}\}^T \{\bar{b}\} \, d\mathcal{V} - \int_{\partial \mathbf{D}_e^u} \{\bar{w}\}^T \{\bar{\lambda}_A\} \, d\mathcal{A} = 0, \quad \forall \bar{w} \in \mathcal{U}^0$$

$$- \int_{\partial \mathbf{D}_e^u} \{\bar{r}_A\}^T (\{\bar{u}\} - \{\bar{u}^*\}) \, d\mathcal{A} = 0, \quad \forall \bar{r}_A \in \mathcal{L}_A^0 \tag{52}$$

$$\int_{\mathbf{D}} ([L_C^*]\{\bar{\omega}\})^T \, [\hat{\mathbf{C}}^{*S}] \, ([L_C^*]\{\bar{\varphi}\}) \; d\mathcal{V} + \int_{\mathbf{D}} (-[\mathrm{e}]\{\bar{\omega}\})^T \, [\hat{\mathbf{A}}^S] \, ([L_A]\{\bar{u}\}) \; d\mathcal{V} + \tag{53}$$

$$+ \int_{\mathbf{D}} (-[\mathrm{e}]\{\bar{\omega}\})^T \, [\hat{\mathbf{A}}^S] \, (-[\mathrm{e}]\{\bar{\omega}\}) \; d\mathcal{V} - \int_{\partial \mathbf{D}_n^\varphi} \{\bar{\omega}\}^T \{\bar{t}_C\} \, d\mathcal{A} +$$

$$- \int_{\mathbf{D}} \{\bar{\omega}\}^T \{\bar{l}\} \, d\mathcal{V} - \int_{\partial \mathbf{D}_e^\varphi} \{\bar{\omega}\}^T \{\bar{\lambda}_C\} \, d\mathcal{A} = 0, \quad \forall \bar{\omega} \in \mathcal{V}^0$$

$$- \int_{\partial \mathbf{D}^\varphi} \{\bar{r}_C\}^T (\{\bar{\varphi}\} - \{\bar{\varphi}^*\}) \, d\mathcal{A} = 0, \quad \forall \bar{r}_C \in \mathcal{L}_C^0 \tag{54}$$

where $\bar{\lambda}_A$ and $\bar{\lambda}_C$ are, respectively, the Lagrange multipliers for the fields $\bar{u}$ and $\bar{\varphi}$, while $\bar{r}_A \in \mathcal{L}_A^0$ and $\bar{r}_C \in \mathcal{L}_C^0$ are their test functions.

The displacement and micro-rotation fields are approximated with the same MLS shape functions Φ_I, resulting in the following expressions in Voigt notation

$$\{\bar{u}\} = \begin{pmatrix} u_x \\ u_y \\ u_z \end{pmatrix} \simeq \{\bar{u}^h(\bar{x})\} = \sum_{I \in S_n} [\Phi_I(\bar{x})]\{\bar{d}_I^u\} = \sum_{I \in S_n} \begin{pmatrix} \Phi_I & 0 & 0 \\ 0 & \Phi_I & 0 \\ 0 & 0 & \Phi_I \end{pmatrix} \begin{pmatrix} d_{Ix}^u \\ d_{Iy}^u \\ d_{Iz}^u \end{pmatrix} \tag{55}$$

$$\{\bar{\varphi}\} = \begin{pmatrix} \varphi_x \\ \varphi_y \\ \varphi_z \end{pmatrix} \simeq \{\bar{\varphi}^h(\bar{x})\} = \sum_{I \in S_n} [\Phi_I(\bar{x})]\{\bar{d}_I^\varphi\} = \sum_{I \in S_n} \begin{pmatrix} \Phi_I & 0 & 0 \\ 0 & \Phi_I & 0 \\ 0 & 0 & \Phi_I \end{pmatrix} \begin{pmatrix} d_{Ix}^\varphi \\ d_{Iy}^\varphi \\ d_{Iz}^\varphi \end{pmatrix} \tag{56}$$

where the terms d_{Ii}^u and d_{Ii}^φ are the nodal parameters of the fields $\bar{u}$ and $\bar{\varphi}$, respectively, and S_n is the set of *support nodes* in the neighbourhood of the point $\bar{x}$. The Lagrange multipliers are instead approximated with Lagrange interpolant N_I as

$$\{\bar{\lambda}_A\} \simeq \{\bar{\lambda}_A^h(\bar{x})\} = \sum_{I \in S_n^e} [N_I(\bar{x})]\{\bar{d}_I^{\lambda_A}\} = \sum_{I \in S_n^e} \begin{pmatrix} N_I & 0 & 0 \\ 0 & N_I & 0 \\ 0 & 0 & N_I \end{pmatrix} \begin{pmatrix} d_{Ix}^{\lambda_A} \\ d_{Iy}^{\lambda_A} \\ d_{Iz}^{\lambda_A} \end{pmatrix} \tag{57}$$

$$\{\bar{\lambda}_C\} \simeq \{\bar{\lambda}_C^h(\bar{x})\} = \sum_{I \in S_n^e} [N_I(\bar{x})]\{\bar{d}_I^{\lambda_C}\} = \sum_{I \in S_n^e} \begin{pmatrix} N_I & 0 & 0 \\ 0 & N_I & 0 \\ 0 & 0 & N_I \end{pmatrix} \begin{pmatrix} d_{Ix}^{\lambda_C} \\ d_{Iy}^{\lambda_C} \\ d_{Iz}^{\lambda_C} \end{pmatrix} \tag{58}$$

where the terms $d_{Ii}^{\lambda_A}$ and $d_{Ii}^{\lambda_C}$ are the nodal parameters of the fields $\bar{\lambda}_A$ and $\bar{\lambda}_C$, respectively, and S_n^e is the set of *support nodes*, belonging to the essential boundary, in the neighbourhood of the point $\bar{x}$. The test functions $\bar{w}$, $\bar{\omega}$, $\bar{r}_A$ and $\bar{r}_C$ are approximated in the same way as their respective field functions.

Introducing these approximations in the weak form and accounting for the arbitrariness of the test functions, Eqs. (51) and (53) can be rewritten as

$$\sum_{I=1}^{n_t}\sum_{J=1}^{n_t}[K_{IJ}]\begin{pmatrix}\{\bar{d}_J^u\}\\ \{\bar{d}_J^\varphi\}\end{pmatrix}+\sum_{I=1}^{n_t}\sum_{K=1}^{n_\lambda}[G_{IK}]\begin{pmatrix}\{\bar{d}_K^{\lambda_A}\}\\ \{\bar{d}_K^{\lambda_C}\}\end{pmatrix}=\sum_{I=1}^{n_t}\{\bar{F}_I\} \tag{59}$$

while Eqs. (52) and (54) result in

$$\sum_{K=1}^{n_\lambda}\sum_{I=1}^{n_t}[G_{IK}]^T\begin{pmatrix}\{\bar{d}_I^u\}\\ \{\bar{d}_I^\varphi\}\end{pmatrix}=\sum_{K=1}^{n_\lambda}\{\bar{q}_K\} \tag{60}$$

where n_t is the total number of nodes in the domain, and n_λ the total number of nodes in the essential boundary. The operators appearing in the previous equations are defined as in the following

$$[K_{IJ}]=\int_{\mathbf{D}}[B_I]^T[\hat{\mathcal{E}}^S][B_J]\,d\mathcal{V} \tag{61}$$

$$[B_I]=\begin{pmatrix}[L_A][\Phi_I] & -[\mathbf{e}][\Phi_I]\\ [0] & [L_C^*][\Phi_I]\end{pmatrix}, \qquad [\hat{\mathcal{E}}^S]=\begin{pmatrix}[\hat{\mathbf{A}}^S] & [0]\\ [0] & [\hat{\mathbf{C}}^{*S}]\end{pmatrix} \tag{62}$$

$$[G_{IK}]=\begin{pmatrix}-\int_{\partial\mathbf{D}_e^u}[\Phi_I]^T[N_K]\,d\mathcal{A} & [0]\\ [0] & -\int_{\partial\mathbf{D}_e^\varphi}[\Phi_I]^T[N_K]\,d\mathcal{A}\end{pmatrix} \tag{63}$$

$$\{\bar{F}_I\}=\begin{pmatrix}\int_{\partial\mathbf{D}_n^u}[\Phi_I]^T\{\bar{t}_A\}\,d\mathcal{A}+\int_{\mathbf{D}}[\Phi_I]^T\{\bar{b}\}\,d\mathcal{V}\\ \int_{\partial\mathbf{D}_n^\varphi}[\Phi_I]^T\{\bar{t}_C\}\,d\mathcal{A}+\int_{\mathbf{D}}[\Phi_I]^T\{\bar{l}\}\,d\mathcal{V}\end{pmatrix} \tag{64}$$

$$\{\bar{q}_K\}=\begin{pmatrix}-\int_{\partial\mathbf{D}_e^u}[N_K]^T\{\bar{u}^*\}\,d\mathcal{A}\\ -\int_{\partial\mathbf{D}_e^\varphi}[N_K]^T\{\bar{\varphi}^*\}\,d\mathcal{A}\end{pmatrix} \tag{65}$$

Introducing the arrays $\{U\}$, $\{\lambda\}$, $\{F\}$ and $\{q\}$ collecting the different nodal parameters $\{\bar{d}_I^u\}$, $\{\bar{d}_I^\varphi\}$, $\{\bar{d}_I^{\lambda_A}\}$, $\{\bar{d}_I^{\lambda_C}\}$, $\{F_I\}$ and $\{q_I\}$ of all the nodes of the model, Eqs. (59) and (60) can be condensed in the global equation

$$\begin{pmatrix}[K] & [G]\\ [G]^T & [0]\end{pmatrix}\begin{pmatrix}\{U\}\\ \{\lambda\}\end{pmatrix}=\begin{pmatrix}\{F\}\\ \{q\}\end{pmatrix} \tag{66}$$

5 NUMERICAL RESULTS

The combination of the proposed micropolar scalar damage models with the Element Free Galerkin method, and their implementation in the **INSANE** system, are illustrated with the numerical simulation of the experimental test of Fig. 1(a) (Winkler et al., 2004).
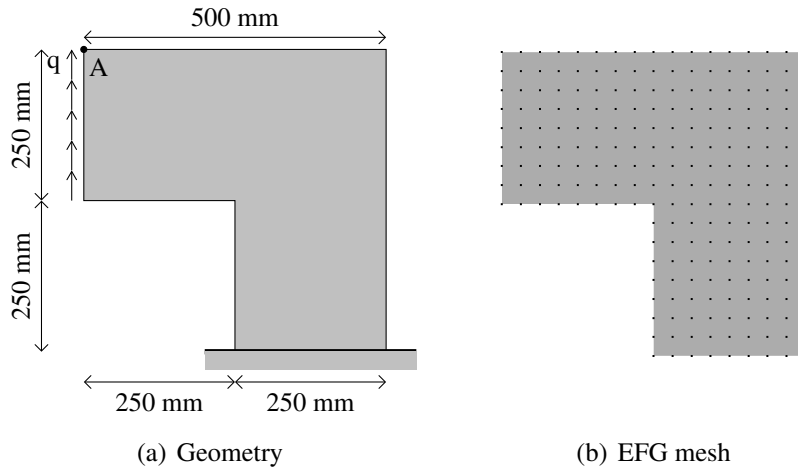
(a) Geometry

(b) EFG mesh

Figure 1: L-shaped panel

The material is characterized by an elastic modulus E = 25850 N/mm^2, a Poisson's modulus ν = 0.18, tensile and compressive uniaxial strengths f$_t$ = 2.70 N/mm^2 and f$_c$ = 31.00 N/mm^2, and a fracture energy G$_f$ = 0.065N/mm^2. The Cosserat's shear modulus is assumed to be α = 2000 N/mm^2, while two bending lengths are considered, L$_f$ = 5 mm and L$_f$ = 10 mm. The coefficients of the damage laws are resumed in Table 1

Table 1: Damage laws parameters

	Mazars		Simplified Mazars
A_t	0.90	χ	0.95
A_c	1.00	β	1100
B_t	4750	K_0	1.05×10^{-4}
B_c	1950		
K_0	7.0×10^{-5}		

The EFG model (Fig. 1(b)) consists in 225 regulary spaced nodes, with linear basis functions and cubic spline weighting functions; the square influence domains at each node have sides of approximately 2.1 times the nodal spacing. The analysis model is a plane-stress state, with a thickness of 100 mm. The loading process is driven by the *generalized displacement control method* (Yang and Shieh, 1990), assuming a reference load q = 28 N/mm, loading factor increments of 0.02 and a tollerance for the convergence in displacement of 1×10^{-4}.

The results of the analysis are presented, for both the *Mazars* and the *simplified Mazars* damage models, in Fig. 2, where the relation between the vertical displacement of the top left point and the load factor is presented (point A in Fig. 1(a)).

In the same figure, the experimental data obtained by Winkler et al. (2004) are also reported. As it can be observed, both the models are in good agreement with the experimental values, regarding the load factor peak. The post-peak behaviour is well represented by the simplified model, while the original Mazars damage law presents a faster degradation of the material
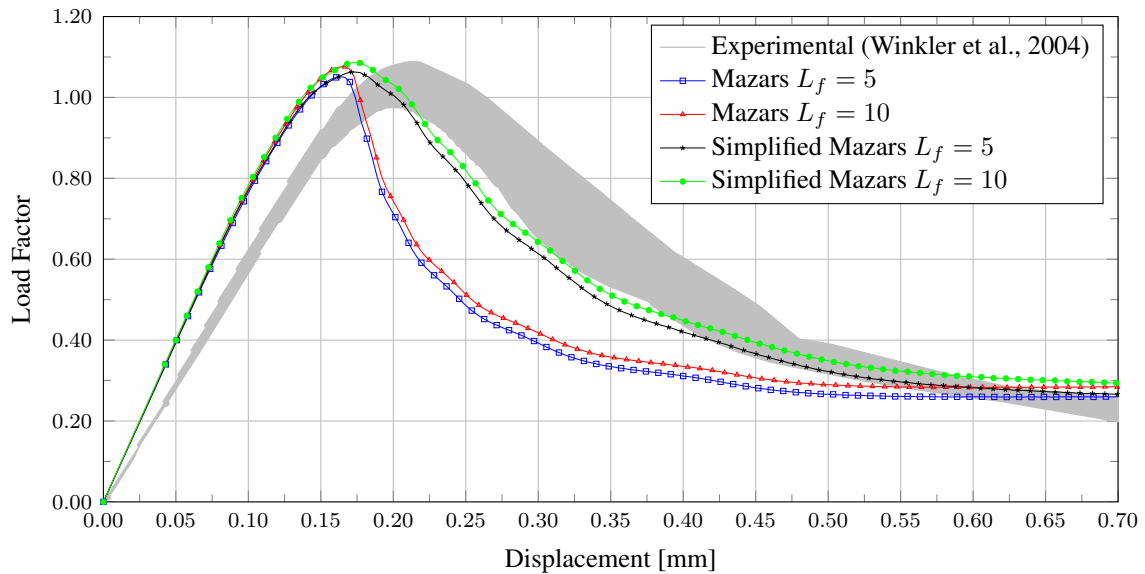
Figure 2: L-shaped panel - Equilibrium paths

properties. Both the models present an initial stiffness higher than the one observed in the experiment; however, this issue is common to all the simulations of such a test that can be found in the literature, and it can be observed also in the original paper of Winkler et al. (2004).

In Fig. 3 the damage distribution corresponding to a vertical displacement of the top left point (point A in Fig. 1(a)) equal to 27 mm is represented, for both the Mazars and the simplified Mazars models, assuming a bending length L_f = 5 mm.
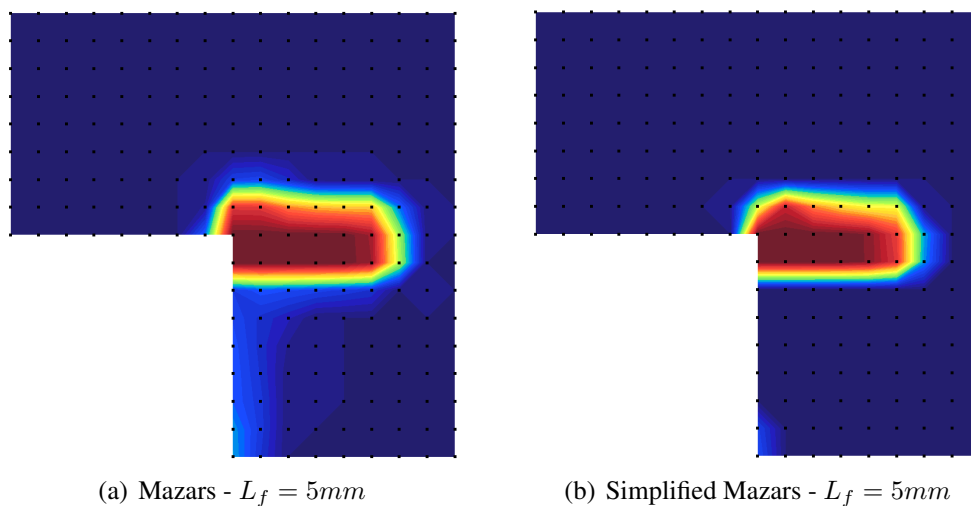

(a) Mazars - $L_f = 5mm$

(b) Simplified Mazars - $L_f = 5mm$

Figure 3: Damage distribution at d_y = 0.27 mm (point A in Fig. 1(a))

6 CONCLUSIONS

The theoretical and computational framework for micropolar scalar damage models proposed in a previous paper (Gori et al., 2015c, 2016), and implemented in the **INSANE** system,

has been extended in order to accomodate additional damage models. The proposed models and their combination with the Element Free Galerkin method have been evaluated with the numerical simulation of an experimental test, showing a good agreement with the empirical results. As discussed in the introduction, both the micropolar theory and the mesh-free approximation methods are capable to regularize the behaviour of numerical simulations where localization occours. However, as pointed out by a number of authors, the regularization effect of both the methods is not effective in a number of situations. Hence, the coupling of the EFG method with the micropolar theory, described in this paper, could represent the basis for future analyses that should be devoted to the investigation of the regularization effects introduced by the different methods and their interaction.

ACKNOWLEDGEMENTS

REFERENCES

Andrade, M. P. & Silva, R. P., 2015. Implementação de bibliotecas de Álgebra linear numérica via interface nativa no INSANE. In *Proceedings of the XXXVI Ibero-Latin American Congress on Computational Methods in Engineering*, Rio de Janeiro, Brazil. ABMEC - Brazilian Association of Computational Methods in Engineering. (in portuguese).

Bauer, S., Dettmer, W., Perić, D., & Schäfer, M., 2012. Micropolar hyper-elastoplasticity: constitutive model, consistent linearization, and simulation of 3D scale effects. *International Journal for Numerical Methods in Engineering*, vol. 91, n. 1, pp. 39–66.

Belytschko, T., Lu, Y. Y., & Gu, L., 1994. Element-free Galerkin methods. *International Journal for Numerical Methods in Engineering*, vol. 37, n. 2, pp. 229–256.

Chen, J. S., Hu, W., Puso, M., & Zhang, X., 2007. Strain smoothing for stabilization and regularization of Galerkin meshfree. vol. 57, pp. 57 – 75.

Chen, J. S., Wu, T. C., & Belytschko, T., 2000. Regularization of material instabilities by mesh-free approximations with intrinsic length scales. *International Journal for Numerical Methods in Engineering*, vol. 47, pp. 1303–1322.

Chen, J. S., Zhang, X., & Belytschko, T., 2004. An implicit gradient model by a reproducing kernel strain regularization in strain localization problems. *Computer Methods in Applied Mechanics and Engineering*, vol. 193, pp. 2827–2844.

Cosserat, E. & Cosserat, F., 1909. *Théorie des corps déformables*. Hermann et fils, Paris. (in french).

Davis, T. A., 2004. A column pre-ordering strategy for the unsymmetric-pattern multifrontal method. *ACM Transactions on Mathematical Software*, vol. 30, n. 2, pp. 165–195.

Davis, T. A., 2006. *Direct Methods for Sparse Linear Systems*. SIAM.

de Borst, R., 1993. A generalization of J2-flow theory for polar continua. *Computer Methods in Applied Mechanics and Engineering*, vol. 103, pp. 347–362.

de Borst, R. & Gutiérrez, M. A., 1999. A unified framework for concrete damage and fracture models including size effects. *International Journal of Fracture*, vol. 95, n. 1-4, pp. 261–277.

de Borst, R. & Sluys, L. J., 1991. Localization in a Cosserat continuum under static and dynamic loading. *Computer Methods in Applied Mechanics and Engineering*, vol. 90, n. 1-3, pp. 805–827.

Gori, L., Penna, S. S., & Pitangueira, R. L. S., 2016. An enhanced tensorial formulation for elastic degradation in micropolar continua. *Applied Mathematical Modelling*, vol. , pp. –. (in press).

Gori, L., Pitangueira, R. L. S., Penna, S. S., & Fuina, J. S., 2015a. A generalized elasto-plastic micro-polar constitutive model. *Applied Mechanics and Materials*, vol. 798, pp. 505–509.

Gori, L., Pitangueira, R. L. S., Penna, S. S., & Fuina, J. S., 2015b. Isotropic damage models based on a generalized micro-polar continuum theory. In *Anais do 57 Congresso Brasileiro do Concreto*, Bonito, Brazil. IBRACON - Instituto Brasileiro do Concreto.

Gori, L., Pitangueira, R. L. S., Penna, S. S., & Fuina, J. S., 2015c. A theoretical and computational framework for isotropic damage models based on a generalized micro-polar continuum theory. In *Proceedings of the XXXVI Ibero-Latin American Congress on Computational Methods in Engineering*, Rio de Janeiro, Brazil. ABMEC - Brazilian Association of Computational Methods in Engineering.

INSANE Project, 2016. `https://www.insane.dees.ufmg.br/`.

Iordache, M. M. & Willam, K., 1998. Localized failure analysis in elastoplastic Cosserat continua. *Computer Methods in Applied Mechanics and Engineering*, vol. 121, n. 3-4, pp. 559–586.

Li, S., Hao, W., & Liu, W. K., 2000. Mesh-free simulations of shear banding in large deformation. *International Journal of Solids and Structures*, vol. 37, pp. 7185–7206.

Li, S. & Liu, W. K., 2000. Numerical simulations of strain localization in inelastic solids using mesh-free methods. *International Journal for Numerical Mehods in Engineering*, vol. 48, pp. 1285–1309.

Liang, K.-Z. & Huang, F.-Y., 1996. Boundary element method for micropolar elasticity. *International Journal of Engineering Science*, vol. 34, n. 5, pp. 509 – 521.

Liu, W. K., Hao, S., Belytschko, T., Li, S. F., & Chang, C. T., 1999. Multiple scale meshfree methods for damage fracture and localization. *Computational Material Science*, vol. 16, pp. 197–205.

Mariano, P. M. & Stazi, F. L., 2005. Computational aspects of the mechanics of complex materials. *Archives of Computational Methods in Engineering*, vol. 12, n. 4, pp. 391–478.

Mazars, J., 1984. *Application de le Mécanique de l'endommagement au comportement non lineaire et à la rupture du béton de Structure*. PhD thesis, Université Pierre et Marie Curie - Laboratoire de Mécanique et Technologie, Paris, France. (in french).

Mazars, J. & Cabot, J. P., 1989. Continuum damage theory - application to concrete. *Journal of Engineering Mechanics*, vol. 115, n. 2, pp. 345–365.

Pozo, P. L., Campos, A., Lascano, S., Oller, S., & Rodriguez-Ferran, A., 2014. A finite points method approach for strain localization using the gradient plasticity formulation. *Mathematical Problems in Engineering*, vol. 2014.

Rahaman, M., Deepu, S., Roy, D., & Reddy, J., 2015. A micropolar cohesive damage model for delamination of composites. *Composite Structures*, vol. 131, pp. 425 – 432.

Silva, R. P., 2012. *Análise não-linear de estruturas de concreto por meio do método Element Free Galerkin*. PhD thesis, UFMG – Federal University of Minas Gerais, Belo Horizonte, Brazil. (in portuguese).

Sluys, L. J., 1992. *Wave propaation, localization and dispersion in softening solids*. PhD thesis, Technische Universiteit Delft, Delft, The Nederlands.

Steinmann, P., 1995. Theory and numerics of ductile micropolar elastoplastic damage. *International Journal for Numerical Methods in Engineering*, vol. 38, pp. 583–606.

Wang, D. & Li, Z., 2012. A two-level strain smoothing regularized meshfree approach with stabilized conforming nodal integration for elastic damage analysis. *International Journal of Damage Mechanics*, vol. 22, n. 3, pp. 440–459.

Winkler, B., Hofstetter, G., & Lehar, H., 2004. Application of a constitutive model for concrete to the analysis of a precast segmental tunnel lining. *International Journal for Numerical and Analytical Methods in Geomechanics*, vol. 28, n. 7-8, pp. 797–819.

Xotta, G., Beizaee, S., & Willam, K. J., 2016. Bifurcation investigation of coupled damage-plasticity models for concrete materials. *Computer Methods in Applied Mechanics and Engineering*, vol. 298, pp. 428–452.

Yang, Y. B. & Shieh, M. S., 1990. Solution method for nonlinear problems with multiple critical points. *AIIA Journal*, vol. 28, n. 12, pp. 2110–2116.